

Normal transport and excitonic condensation in an incoherent semimetal

Geo Jose¹, Kangjun Seo², Bruno Uchoa¹

¹*Center for Quantum Research and Technology, Department of Physics and astronomy,
University of Oklahoma, Norman, Oklahoma 73019, USA and*

²*School of Electrical and Computer Engineering,
The University of Oklahoma, Tulsa, OK 74135, USA*

(Dated: March 8, 2022)

We study a two-band dispersive SYK model in $1 + 1$ dimension at half filling. We suggest a model that describes a semimetal with quadratic dispersion at half-filling. We compute the Green's function at the saddle point using a combination of analytical and numerical methods. Employing a scaling symmetry of the Schwinger Dyson equations that becomes transparent in the strongly dispersive limit, we show that the exact solution of the problem yields a distinct type of non-Fermi liquid with sublinear $\rho \propto T^{2/5}$ temperature dependence of the resistivity. A scaling analysis indicates that this state corresponds to the fixed point of the dispersive SYK model for a quadratic band touching semimetal. We examine the formation of indirect exciton condensation in a bilayer system constructed from the above model. We find that the condensation temperature scales as a fast power-law $T_c \propto g^5$, with g the strength of the repulsive coupling between the layers.

I. INTRODUCTION

Sachdev-Ye-Kitaev (SYK _{q}) models describe strongly interacting fermions with infinite range, q -body, random all-to-all interactions. The $0 + 1$ dimensional SYK _{q} dot model [1, 2] exhibits an approximate conformal symmetry in the infrared, is exactly solvable in the limit of a large number of fermion flavors, saturates the bound on quantum chaos and are dual to gravitational theories in $1 + 1$ dimensions. [3–5]. Useful connections to the black hole information problem have also been established [6].

In these models, approximate conformal symmetry in the strong coupling/low frequency regime leads to power law behavior of correlation functions. In the SYK₄ model, the zero temperature two-point correlation function decays as $G(\omega) \sim 1/\sqrt{\omega}$. Finite temperature Green's functions can be then obtained by appealing to conformal symmetry [1]. In dispersive versions of the SYK model, they result in the linear temperature dependence of the dc resistivity, $\rho \propto T$, a characteristic feature of strange metal phases. It was originally conjectured that the linear scaling of the scattering rate in the strange metal phase was due to hyperscaling in the proximity of a quantum critical point buried inside the superconducting phase. Recent momentum resolved electron energy spectroscopy experiments in the cuprates revealed the emergence of a mysterious momentum independent energy scale nearly one order of magnitude larger than the temperature range of the quantum critical fan [7, 8], at odds with conventional quantum critical theories. One may speculate [9–13] that the origin of the strange metal phase could be related to aspects of the physics of incoherent metals.

Various lattice generalizations [13–18] of the dot model comprising of connected SYK dots have been recently proposed in the regime where the SYK coupling is the dominant energy scale of the problem. The general idea behind many of those extensions is to build on the solution of the dot model including lattice effects perturba-

tively. Weakly dispersive versions of the SYK model were used to describe incoherent or ‘Plankian’ metals which lack well defined quasiparticles [12, 19, 20]. These incoherent metals typically have a crossover between the incoherent high temperature regime and a low temperature Fermi liquid behavior [16]. The crossover energy scale between the two regimes is set by t^2/J , with t proportional to the band width and $J \gg t$ the SYK coupling. In the low temperature regime, the coherence of the quasiparticles is restored by the presence of a large Fermi surface. Semimetals, on the other hand, abridge a large class of gapless multiband systems that lack a Fermi surface. One could ask what is the nature of the normal state in a disordered semimetal with random local couplings.

Motivated by these ideas, we study a 1D ladder with local random couplings at every unit cell, as shown in Fig. 1. The hopping amplitudes between lattice sites is finely tuned such that this system describes a half-filled semimetal with quadratic dispersion and local SYK couplings. The weakly dispersive limit $t^2/J \ll \omega \ll J$ has approximate conformal invariance and recovers the usual

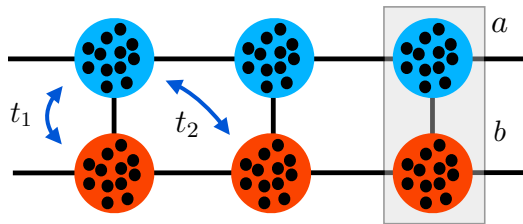


Figure 1. Dispersive SYK ladder model: The unit cell contains two sites, one for each chain (color). Each color site hosts N complex fermions, which interact locally through random couplings. We assume that hopping is only allowed between different color sites, with t_1 the NN hopping and t_2 the NNN one. The two-band quadratic dispersion in (3) can be obtained by tuning $t_1 = -2t_2 = t$, with $m = 2/(ta^2)$ the effective mass of the fermions, where a is the lattice constant.

SYK transport behavior, as expected. In the strongly dispersive regime, $\omega \ll t^2/J$, where the bandwidth of the conduction electrons can be large, the scaling symmetry of the problem becomes transparent, albeit the absence of conformal symmetry. In this limit, the incoherent regime extends to down zero frequency and temperature, unlike in the more conventional metallic case. We show that the resistivity of this model has a sublinear scaling with temperature,

$$\rho \propto T^{2/5}, \quad (1)$$

whereas the Lorentz ratio $L = \kappa/(\sigma T) \approx 3.2$ is fairly close to the value expected for a Fermi liquid, $L = \pi^2/3$. We find though a scaling argument that when the system starts from the SYK fixed point at high temperature, it flows towards a distinct non-Fermi liquid (NFL) fixed point at zero temperature. At intermediate energy scales, away from the low temperature fixed point, the system crosses over from a “Plankian” semimetal to an incoherent NFL with sublinear temperature scaling of the resistivity.

We finally address the emergence of excitonic condensation in two copies of SYK quantum dot ladders coupled to each other in the particle hole channel. Evidence of indirect excitonic condensation has been experimentally observed in transition metal dichalcogenides [21] and in the Landau levels of double bilayer graphene in the quantum Hall regime [22]. As superconductivity [23–26], excitonic condensation may have unusual features in incoherent systems. We find that in the infinite bandwidth limit, the critical temperature scales with the coupling g in the particle-hole channel with a fast power law,

$$T_c \propto \frac{g^5}{J^6}. \quad (2)$$

This paper is organized in the following way: in section II we introduce the lattice model of a 1D ladder of SYK quantum dots that behaves as a 1D semimetal with quadratic dispersion. In section III we address the Green’s function of this system at zero and finite temperature. In the infinite bandwidth limit ($J \ll t$), where conformal symmetry is not present, we numerically extract the finite temperature scaling functions of the Green’s function and of the self-energy. In section IV, we discuss a scaling analysis of the problem and the crossover between the high temperature incoherent Plankian regime and the low temperature NFL one. In section V we address the temperature scaling of the dc resistivity of the model. In section VI, we discuss the possibility of excitonic condensation of an incoherent semimetal in the low temperature NFL regime. Finally, in section VII we present our conclusions.

II. MODEL

We consider N –flavors of complex fermions hopping on an 1D lattice. Each lattice site hosts an SYK dot with random, site dependent interactions J_{ijkl}^x between them. The indexes $i, j, k, \ell = 1, \dots, N$ label the N –flavors/colors per site. We start from a 1D ladder shown in Fig. 1, with

two sites per unit cell, shown in blue and red. Allowing hopping processes between blue and red sites only, the Hamiltonian of the kinetic term can be written as

$$\hat{\mathcal{H}}_0 = \int_k \sum_{\nu} f(k) \psi_{k,i,\nu}^{\dagger} (\sigma_x)_{\nu,\nu'} \psi_{k,i,\nu'}, \quad (3)$$

where

$$f(k) = t_1 + 2t_2 \cos(ka), \quad (4)$$

with t_1 and t_2 the hopping between nearest neighbors (NN) and second nearest neighbors (NNN) respectively among different color sites, and $f_k \equiv a(2\pi)^{-1} \int_{-\Lambda}^{\Lambda} dk$ with $\Lambda = \pi/a$ the ultraviolet cutoff. $\psi_{i,\nu}$ is a two-component spinor in the site basis of the unit cell $\nu = a, b$ and σ_x is the real off-diagonal Pauli matrix in that basis. Fine tuning the hopping constants to $t_1 = -2t_2 = t$, then

$$\mathcal{H}_0 = \int_k \sum_{i\nu} \frac{k^2}{2m} \psi_{k,i,\nu}^{\dagger} (\sigma_x)_{\nu\nu'} \psi_{k,i,\nu'}, \quad (5)$$

in the continuum limit ($k \ll 1/a$), with $m^{-1} = ta^2/2$. In the following, we set $a \rightarrow 1$.

These fermions interact via a local, instantaneous two body SYK interaction,

$$\mathcal{H}_{\text{SYK}} = \frac{1}{(N)^{\frac{3}{2}}} \sum_{i\nu', jkl} \int_x J_{ijkl}^x \psi_{x,i,\nu}^{\dagger} \psi_{x,j,\nu'}^{\dagger} \psi_{x,k,\nu'} \psi_{x,\ell,\nu}, \quad (6)$$

with random, color site independent matrix elements J_{ijkl}^x that are properly antisymmetrized with $J_{ijkl}^x = -J_{jikl}^x = -J_{ijlk}^x$. As in the other SYK models, we take these to be complex Gaussian distributed coupling with a zero mean value $\langle \langle J_{ijkl}^x \rangle \rangle = 0$ and variance $\langle \langle |J_{ijkl}^x|^2 \rangle \rangle = J^2/4$.

The standard method to study the current problem is the imaginary time path integral formalism, where the partition function is given by $\mathcal{Z} = \int [\mathcal{D}\bar{\psi} \mathcal{D}\psi] e^{-S}$, where $S = S_0 + S_{\text{SYK}}$, with

$$S_0 = \int_{\tau,x} \sum_{\ell,\nu} \bar{\psi}_{\ell,\nu}(\tau,x) \left[\partial_{\tau} - (\sigma_x)_{\nu\nu'} \frac{\partial_x^2}{2m} \right] \psi_{\ell,\nu'}(\tau,x). \quad (7)$$

We define $\int_{\tau} \equiv \int_0^{\beta} d\tau$, with $\beta = 1/T$, and S_{SYK} the corresponding two body action of (6) with same time Grassmann fields $\bar{\psi}(\tau, x)$ and $\psi(\tau, x)$. In order to deal with the disorder, we use the replica trick and average over disorder realizations, where

$$\langle \langle e^{-\sum_{ijkl} J_{ijkl} A_{ijkl}} \rangle \rangle = e^{2J^2 \sum_{ijkl} \bar{A}_{ijkl} A_{ijkl}}. \quad (8)$$

Defining the Green’s function

$$\hat{G}_{\nu\nu'}(\tau, x) = -\frac{1}{N} \sum_{\ell=1}^N \langle T[\psi_{\nu,\ell}(0,0) \bar{\psi}_{\nu',\ell}(x,\tau)] \rangle, \quad (9)$$

the integration over the fermionic fields results in the saddle point action,

$$\mathcal{S}_{\text{eff}} = -\log \det \left[\delta(\tau - \tau') \delta(x - x') \left(\partial_\tau + \sigma_x (i\partial_x)^2 \right) + \hat{\Sigma}(x - x', \tau - \tau') \right] - \frac{J^2}{2} \int_{\tau, \tau'} \text{tr} \hat{G}^2(0, \tau - \tau') \text{tr} \hat{G}^2(0, \tau' - \tau) - \int_{x, x'} \int_{\tau, \tau'} \text{tr} \left[\hat{\Sigma}(x - x', \tau - \tau') \hat{G}(x' - x, \tau' - \tau) \right], \quad (10)$$

where $\hat{\Sigma}(x - x', \tau - \tau')$ is the self-energy. The action can be minimized exactly in \hat{G} and $\hat{\Sigma}$ in the large- N limit. Following the minimization, the solutions form a set of Schwinger-Dyson equations

$$\hat{G}^{-1}(i\omega_n, k) = i\omega_n - \frac{k^2}{2m} \sigma_x - \hat{\Sigma}(i\omega_n, k), \quad (11)$$

and

$$\hat{\Sigma}(\tau, x) = -J^2 \delta(x) \hat{G}(-\tau, 0) \text{tr} \left[\hat{G}(\tau, 0) \hat{G}(\tau, 0) \right], \quad (12)$$

The self-energy $\hat{\Sigma}(i\omega_n, k) \equiv \hat{\Sigma}(i\omega_n)$ is therefore momentum independent, reflecting the x -dependence of the couplings $J_{ijk\ell}^x$. The disorder averaged SYK term is uncorrelated and purely local. We denote the Fourier transform of the momentum independent self-energy as $\hat{\Sigma}(\tau)$. We also denote

$$\hat{G}(\tau) \equiv \hat{G}(\tau, 0) = \int_k \hat{G}(\tau, k) \quad (13)$$

for the momentum integrated Green's function.

III. GREEN'S FUNCTION

If one takes the ansatz for the Green's function, $\hat{G}(\tau) = \mathcal{G}(\tau) \sigma_x$, the self energy then has to be of the form $\hat{\Sigma}(\tau) = \Sigma(\tau) \sigma_x$. As in usual SYK models, we make the usual infrared assumption $i\omega_n \ll \Sigma(i\omega_n)$. The Schwinger Dyson equations (11) and (12) can be written as

$$\begin{aligned} \mathcal{G}(i\omega_n) &= - \int_k \frac{1}{\frac{k^2}{2m} + \Sigma(i\omega_n)} \\ &= - \frac{\sqrt{2m}}{\pi \sqrt{\Sigma(i\omega)}} \tan^{-1} \left(\frac{\Lambda}{\sqrt{2m} \sqrt{\Sigma(i\omega)}} \right), \end{aligned} \quad (14)$$

and

$$\Sigma(\tau) = -J^2 \mathcal{G}^2(\tau) \mathcal{G}(-\tau), \quad (15)$$

There are two limits of particular interest. As it will be clear in the next section, one is the intermediate frequency limit $t^2/J \ll \omega \ll J$, where the argument of the $\tan^{-1}(y)$ function,

$$y \equiv \frac{\Lambda}{\sqrt{2m} \sqrt{\Sigma(i\omega)}} \quad (16)$$

is small. This regime corresponds to the weakly dispersive limit, which recovers the physics of the $0 + 1$ dimensional SYK dot. The other is the strongly dispersive regime, $\omega \ll t^2/J$, where $y \gg 1$. We show that this limit is exactly solvable and leads to a different NFL regime.

A. Weakly dispersive limit

In this weakly dispersive limit ($y \ll 1$), the SYK physics dominates and typically one obtains a fully incoherent system with a linear in T dc resistivity. In that regime, Eq. (14) becomes

$$\mathcal{G}(i\omega_n) \approx -\frac{1}{\pi} \frac{\Lambda}{\Sigma(i\omega_n)}, \quad (17)$$

Eq. (15) and (17) have the form of the SYK dot model [1]. These equations have conformal/reparametrization invariance, indicating a power law solution at $T = 0$.

At zero temperature, those two equations can be solved by the ansatz $\mathcal{G}(i\omega) = c_1 e^{-i\frac{\pi}{4}} \omega^{-\frac{1}{2}}$ [1]. Using this result in Eq. (15) and taking a Fourier transform one finds

$$\Sigma(i\omega) = -\frac{J^2 c_1^3}{\pi} e^{i\frac{\pi}{4}} \sqrt{\omega}, \quad (18)$$

where the constant $c_1 = \Lambda^{\frac{1}{4}} / \sqrt{J}$. The zero temperature dispersive Green's function is

$$G(i\omega, k) = \frac{1}{\Sigma(i\omega)} - \frac{k^2/2m}{\Sigma(i\omega)^2} + \dots \quad (19)$$

This solution introduces a perturbative correction to the SYK Green's function, in the same spirit as in the metallic case.

To get the finite temperature solutions, one can then use the conformal map, $\tau \rightarrow f(\tau) = \tan \frac{\pi\tau}{\beta}$. Applying this to the Fourier transform of $\mathcal{G}(i\omega)$ gives

$$\mathcal{G}(\tau) = \text{sgn}(\tau) c_1 \sqrt{\frac{1/\beta}{2 \sin \pi\tau/\beta}}. \quad (20)$$

$\Sigma(i\omega_n)$ can then be obtained from a Fourier transform of (15),

$$\Sigma(i\omega_n) = iJ^2 c_1^3 \frac{(2\pi)^{3/2} \sqrt{2} \Gamma \left(\frac{3}{4} + \frac{\omega_n \beta}{2\pi} \right) \Gamma \left(-\frac{1}{2} \right)}{\sqrt{\beta} \pi \Gamma \left(\frac{1}{4} + \frac{\omega_n \beta}{2\pi} \right)}. \quad (21)$$

The dispersive Green's function at finite temperature is

$$G(i\omega_n, k) = \frac{1}{\Sigma(i\omega_n)} - \frac{k^2/2m}{\Sigma^2(i\omega_n)} + \dots \quad (22)$$

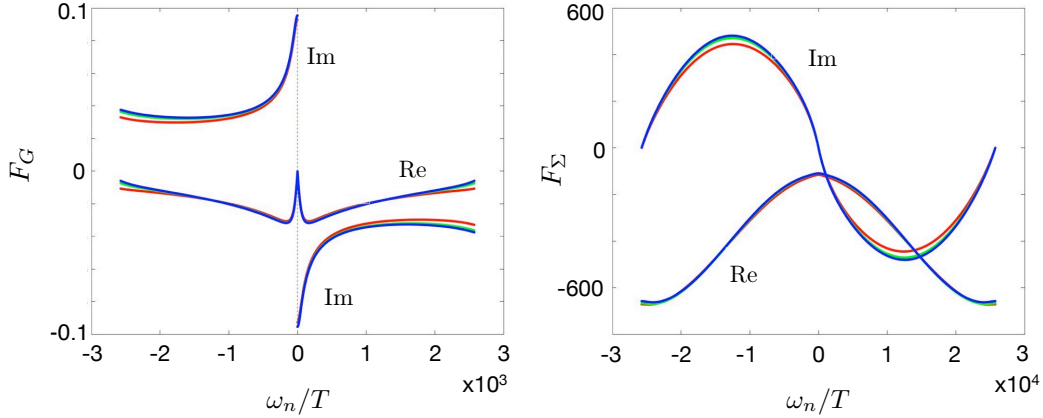


Figure 2. a) Numerical solution for the Green's function and b) for the self-energy. The real and imaginary parts of the scaling function were computed at various temperatures, namely $\beta = 1/T = 256, 64$ and 4 (green line, blue and red, respectively) with β in units of $2m$ with $a \rightarrow 1$. All curves nearly coincide at low frequencies, where the scaling functions are expected to be temperature independent.

B. Strongly dispersive regime

Next we consider the regime where $y \gg 1$. As we will show below, this inequality corresponds to the regime where

$$(i\omega, T) \ll \frac{t^2}{J}, \quad (23)$$

and leads a different kind of NFL behavior compared to weakly dispersive SYK models.

In the $y \gg 1$ regime, the Schwinger-Dyson equation (14) reads

$$\mathcal{G}(i\omega) = -\frac{1}{2} \frac{\sqrt{2m}}{\sqrt{\Sigma(i\omega)}}. \quad (24)$$

Eq. (15) and (24) admit a power law solution at $T = 0$. Analytically continuing to real frequencies, they can be solved by the ansatz

$$\mathcal{G}(\omega) = Ce^{-i\phi} J^{-\frac{2}{5}} m^{\frac{1}{5}} |\omega|^{-\Delta}, \quad (25)$$

where $\Delta = 2/5$, as found in a related model, with

$$C = \left[\frac{\sin(\frac{9\pi}{10}) \pi^2 \Gamma(\frac{9}{5})}{2^{\frac{3}{2}} \sin^3(\frac{11\pi}{20}) \Gamma^3(\frac{3}{5})} \right]^{\frac{1}{5}} \approx 0.79, \quad (26)$$

and $\phi = \frac{11\pi}{20}$. That solution corresponds to a self-energy

$$\Sigma(\omega) = C' e^{-i\phi'} J^{\frac{4}{5}} m^{\frac{3}{5}} |\omega|^{2\Delta} \gg |\omega|, \quad (27)$$

from equation (15), where

$$C' = C^3 \frac{\sin^3(\frac{11\pi}{20}) \Gamma^3(3/5)}{\pi^2 \sin(\frac{9\pi}{10}) \Gamma(9/5)} \approx 0.55, \quad (28)$$

and $\phi' = \frac{9\pi}{20}$. Explicit verification of this solution follows by Fourier transforming

$$\mathcal{G}(\tau) = -\frac{C}{\pi} \sin \phi \Gamma(1 - \Delta) \frac{1}{|\tau|^{1-\Delta}}, \quad (29)$$

and calculating $\Sigma(\omega)$ from (15). The zero-temperature Green's function is hence

$$\hat{G}(\omega, k) = \frac{\sigma_x}{\frac{k^2}{2m} + C' e^{-i\phi'} J^{\frac{4}{5}} m^{\frac{3}{5}} |\omega|^{2\Delta}}, \quad (30)$$

corresponding to a well behaved spectral function $\hat{A}(\omega, k) = -2\text{Im}\hat{G}(\omega, k)$ that does not have singularities. This regime describes a distinct type of incoherent semimetal, and is valid all the way down to zero frequency or temperature. The density of states of the system is

$$\rho(\omega) = -\frac{1}{\pi} \text{Im}\mathcal{G}(\omega) = \frac{C}{\pi} \sin \phi J^{-\frac{2}{5}} m^{\frac{1}{5}} |\omega|^{-\Delta}. \quad (31)$$

It contrasts with the result in the coherent $J \rightarrow 0$ limit of the ladder problem model (restoring $i\omega$ and hence the pole of the Green's function), where the density of states is $\rho(\omega) \propto 1/\sqrt{|\omega|}$.

Note that the linear in T resistivity in SYK models stems from $\Delta = \frac{1}{2}$. In strongly dispersive semimetals, with $\Lambda \gg J$, finite temperature solutions cannot be obtained using a conformal map on the $T = 0$ solution because (15) and (24) do not have the requisite conformal/reparametrization symmetry. Finite temperature solutions to these equations then have to be obtained numerically. However, we still have a scaling symmetry which dictates a certain scaling form for the solutions.

Rewriting (24) in τ -space,

$$\int_{\tau_1, \tau_2} \mathcal{G}(\tau) \mathcal{G}(\tau - \tau_2) \Sigma(\tau - \tau_1) = \frac{m}{2} \delta(\tau). \quad (32)$$

It is easy to see that these equations are invariant under

$$\tau \rightarrow b\tau, \quad \mathcal{G} \rightarrow b^{-\frac{3}{5}}\mathcal{G}, \quad \Sigma \rightarrow b^{-\frac{9}{5}}\Sigma. \quad (33)$$

Under this scaling, $T \rightarrow T/b$ leaving $T\tau$ invariant. With this information, one can see that (15) and (24) admit a solution of the form

$$\mathcal{G}(\tau) = m^{\frac{1}{5}}J^{-\frac{2}{5}}T^{\frac{3}{5}}\tilde{\mathcal{G}}(T\tau) \quad (34)$$

and

$$\Sigma(\tau) = m^{\frac{3}{5}}J^{\frac{4}{5}}T^{\frac{9}{5}}\tilde{\Sigma}(T\tau). \quad (35)$$

Equivalently in Fourier space, we find

$$\mathcal{G}(i\omega_n) = m^{\frac{1}{5}}(JT)^{-\frac{2}{5}}F_G\left(\frac{\omega_n}{T}\right) \quad (36)$$

$$\Sigma(i\omega_n) = m^{\frac{3}{5}}(JT)^{\frac{4}{5}}F_\Sigma\left(\frac{\omega_n}{T}\right) \quad (37)$$

where $F_{G,\Sigma}$ are scaling functions that are independent of temperature T and the coupling J , with ω_n a Matsubara frequency. The dispersive finite temperature Green's function of the problem in this regime is

$$\hat{G}^{-1}(i\omega_n, k) = -\left(\frac{k^2}{2m} + m^{\frac{3}{5}}(JT)^{\frac{4}{5}}F_\Sigma(\omega_n/T)\right)\sigma_x. \quad (38)$$

As we shall see later, this will suffice for us to determine the temperature dependence of various transport coefficients. Strictly speaking, the scaling symmetry is only present in the infrared limit of the theory. This means that the exact numerical solutions may violate these scaling forms at very high frequencies. The numerically obtained scaling functions are plotted in Figure. 2. The plots show good agreement with Eq. (37) even outside the infrared limit.

IV. SCALING ANALYSIS

After averaging over the disorder, which is spatially uncorrelated, the SYK term in the action has eight fermionic fields, which we symbolically write as

$$\mathcal{S}_{\text{SYK}} = J^2 \int_{\tau_1, \tau_2, x} [\bar{\psi}(\tau_1, x)\psi(\tau_1, x)]^2 [\bar{\psi}(\tau_2, x)\psi(\tau_2, x)]^2. \quad (39)$$

Rescaling time as $\tau' = \tau/s$ and imposing the SYK coupling J to be marginal, then the fields rescale as $\psi' = \psi/s^{\frac{1}{4}}$. As pointed out before [15, 16], analyzing the problem in the vicinity of the fixed point of the $0+1$ dimensional SYK model ($t = 0$), the kinetic term is a relevant perturbation and the hopping parameter grows as $t' = t\sqrt{s}$. If one starts from temperature T in the weakly dispersive regime $t \ll J$, the hopping will grow until $t'(s_*) \sim J$ for a rescaling parameter no larger than $s_* = J/T$. Hence, the scaling stops at $T = t^2/J$. The validity of the incoherent ‘‘Plankian’’ regime requires that

$$T \gg T_* = t^2/J, \quad (40)$$

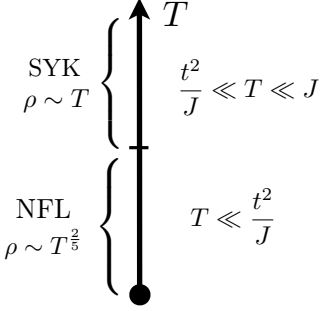


Figure 3. Different temperature regimes in the scaling. At temperature $T > T_* = t^2/J$, the system is close to the $0+1$ dimensional SYK fixed point and shows Plankian behavior, with linear dependence of the resistivity in temperature. Below $T_* = t^2/J$ the system crosses over towards a distinct type of incoherent NFL, with $\rho \sim T^{\frac{2}{5}}$.

as in the case of incoherent metals with a finite Fermi surface [16].

If one continues to lower the temperature further below T_* , we claim that the system crosses over to a different type of incoherent NFL regime with sublinear temperature scaling of the resistivity. From the perspective of the Schwinger-Dyson equations (14) and (15), the parameter that controls the crossover between the weakly and the strongly dispersive regimes is

$$y(T) \sim \sqrt{\frac{t}{\Sigma(T)}}. \quad (41)$$

In the strongly dispersive regime $y(T) \gg 1$, setting $m \sim t^{-1}$, one can write the solution of the finite temperature self-energy (37) as

$$\Sigma(T) \propto t^{-\frac{3}{5}}(JT)^{\frac{4}{5}} \ll t. \quad (42)$$

This inequality leads to $T \ll T_* = t^2/J$. In the same way, in the weakly dispersive regime ($y(T) \ll 1$),

$$\Sigma(T) \propto \sqrt{JT} \gg t, \quad (43)$$

as seen from Eq. (21), implying that $T \gg T_*$.

We note that in the case of metals, the $T < T^*$ regime was found to realize a Fermi liquid. In the case of a 1D half-filled semimetal with parabolic touching, we showed that the low temperature regime does not lead to a semimetal, but to another type of incoherent NFL, whose transport properties will be addressed in the next section.

V. TRANSPORT

In this section, we look at the electric and thermal conductivities using the above finite temperature solutions.

These can be computed using the Kubo formula. The charge current operator for this model is

$$\hat{j}_e = \frac{e}{2m} \int_k \sum_i k \psi_{ki}^\dagger \sigma_x \psi_{ki}. \quad (44)$$

The zero frequency conductivity is given by

$$\sigma_{dc} = \lim_{\omega \rightarrow 0} \frac{\text{Im} \mathcal{K}^{\text{ret}}(\omega)}{\omega}, \quad (45)$$

where $\mathcal{K}^{\text{ret}}(\omega)$ is the retarded current-current correlation function, $\mathcal{K}(\tau) = \langle T[\hat{j}_e(0, x)\hat{j}_e(\tau, x)] \rangle$, given by the series of diagrams in Figure 4. Each diagram displayed in the that figure is of order N . For instance, in diagram (b) each SYK vertex contributes a factor of $N^{-\frac{3}{2}}$, while the three independent flavor sums contribute N^4 , making it a total of order N . Diagrams in (b) and (c) vanish because the current vertex is an odd function of momenta. Since the summation over momenta through each current vertex can be performed independently, that leads to a zero contribution [28]. The remaining diagram is shown in Fig. 4a, which can be written in terms of the Green's functions derived before as

$$\mathcal{K}(i\omega_n) = \frac{Ne^2}{(2m)^2} T \text{tr} \sum_{\nu_n} \int_k k^2 \hat{G}(i\nu_n, k) \hat{G}(i\nu_n + i\omega_n, k). \quad (46)$$

The transport properties of the weakly dispersive regime recovers the expected behavior of incoherent metals found in Ref. [13, 16], $\sigma_{dc} \propto 1/T$, and we will focus instead in the strongly dispersive case.

It is usually challenging to sum over Matsubara frequencies in the absence of poles in the Green's functions. One can circumvent that difficulty by using the spectral representation of the Green's function

$$\hat{G}(i\omega_n, k) = \int_{\omega'} \frac{\hat{A}(k, \omega')}{i\omega_n - \omega'} \quad (47)$$

with

$$\hat{A}(k, \omega) = -\frac{1}{\pi} \sigma_x \text{Im} \frac{1}{\frac{k^2}{2m} + \Sigma(\omega + i0_+)} \quad (48)$$

the spectral function. One arrives at

$$\sigma_{dc} = \frac{Ne^2 \sqrt{2m}}{\pi^2 T} \int_{\omega} \frac{[\text{Im} \Sigma(\frac{\omega}{T})]^2}{\cosh^2(\frac{\omega}{2T})} \int_k \frac{k^2}{\left| \frac{k^2}{2m} + \Sigma(\frac{\omega}{2T}) \right|^4}. \quad (49)$$

Equivalently, casting Eq. (49) in terms of the scaling functions (37), the dc conductivity is

$$\sigma_{dc}(T) = \frac{Ne^2}{\sqrt{2m} (JT)^{\frac{2}{5}}} I_1, \quad (50)$$

where

$$I_1 = \frac{1}{\pi^2} \int_0^\infty dz \frac{[\text{Im} F_\Sigma(z)]^2}{\cosh^2(\frac{z}{2})} \int_0^\infty dy \frac{y^2}{|y^2 + F_\Sigma(z)|^4} \quad (51)$$

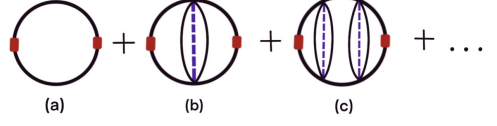


Figure 4. Diagrams that contribute to the current-current correlation function in the large- N limit. Red rectangles represent the current vertex. Black lines represent the fermion Green's function and dotted blue line represents disorder average.

is a dimensionless integral, and $F_\Sigma(z)$ the analytically continued scaling functions of the self energy.

A signature property of Fermi liquids is captured by the Lorentz ratio, $L = \kappa/(\sigma T)$, which is the ratio of thermal (κ) and electric (σ) conductivities. Since we are considering a particle hole symmetric model, thermoelectric effects can be ignored in the computation of κ . The energy current, whose correlation function determines the thermal conductivity, is given by

$$\hat{j}_E = \int_k \sum_i \frac{k}{2m} \psi_{k,i}^\dagger \sigma_x \partial_\tau \psi_{k,i}. \quad (52)$$

In the present particle-hole symmetric case, the thermal conductivity is then given by the same diagrams as in the case of σ . Following the same prescription as above,

$$\kappa = \lim_{\omega \rightarrow 0} \frac{\mathcal{K}_E^{\text{ret}}(\omega)}{\omega T}, \quad (53)$$

where $\mathcal{K}_E(\tau) = \langle T[\hat{j}_E(0, x)\hat{j}_E(\tau, x)] \rangle$ is a thermal current-current correlation function. This leads to

$$\kappa = \frac{Ne^2}{\sqrt{2m} J^{\frac{2}{5}}} T^{\frac{3}{5}} I_2, \quad (54)$$

where

$$I_2 = \frac{1}{\pi^2} \int_0^\infty dz z^2 \frac{\text{Im} [F_\Sigma(z)]^2}{\cosh^2(\frac{z}{2})} \int_0^\infty dy \frac{y^2}{|y^2 + F_\Sigma(z)|^4}. \quad (55)$$

In order to calculate integrals I_1 and I_2 , one needs to perform a numerical analytical continuation of the scaling functions obtained in section III. In the spirit of SYK models, we compute these integrals assuming the scaling form to be valid over the entire range of frequencies. Numerical analytical continuation is a challenging problem. The numerical integrals were done with the Pade approximation method in the TRIQS library [29, 30].

We numerically find that slight variations in the Matsubara scaling forms can significantly affect the integrals I_1 and I_2 , but their ratio is insensitive to numerical issues with the analytical continuation process in the regime of interest. The Lorentz ratio is

$$L = \frac{\kappa}{T\sigma} = \frac{I_2}{I_1} \approx 3.2, \quad (56)$$

which is rather close to the Fermi liquid value of $L_{FL} = \pi^2/3$.

VI. EXCITONIC CONDENSATION

In order to address the presence of excitonic condensation in incoherent semimetals, we consider a version of model (5), where the free Hamiltonian and the SYK term are both written in the particle-hole basis, namely

$$\mathcal{S}_0 = \int_{\tau,x} \sum_{\alpha,\ell,\nu} \bar{\psi}_{\ell,\nu}^{(\alpha)}(\tau,x) \left[\partial_{\tau} - (\sigma_z)_{\nu\nu'} \frac{\partial_x^2}{2m} \right] \psi_{\ell,\nu'}^{(\alpha)}(\tau,x), \quad (57)$$

and

$$\begin{aligned} \mathcal{S}_{\text{SYK}} = & \sum_{\alpha\nu\nu',ijk\ell} \int_x \frac{J_{ijk\ell}^{x,\alpha}}{(2N)^{\frac{3}{2}}} \\ & \times \bar{\psi}_{i,\nu}^{(\alpha)}(\tau,x) \bar{\psi}_{j,\nu'}^{(\alpha)}(\tau,x) \psi_{k,\nu'}^{(\alpha)}(\tau,x) \psi_{\ell,\nu}^{(\alpha)}(\tau,x) \end{aligned} \quad (58)$$

In this basis, the index $\nu = e, h$ describes electrons (e) or hole (h) states, whereas $\alpha = 1, 2$ describes two copies of the ladders, which physically can be described in terms of two layers coupled to each other through an interaction in the particle-hole channel,

$$\begin{aligned} \mathcal{S}_g = & \frac{g}{N} \int_{\tau,x} \sum_{ij} \bar{\psi}_{i,e}^{(1)}(\tau,x) \bar{\psi}_{j,h}^{(2)}(\tau,x) \psi_{j,h}^{(2)}(\tau,x) \psi_{i,e}^{(1)}(\tau,x) \\ & + (1) \leftrightarrow (2). \end{aligned} \quad (59)$$

with $g > 0$. Pairing across the different layers avoids recombination effects that typically destroy condensation of direct excitons.

The total action is $\mathcal{S} = \mathcal{S}_0 + \mathcal{S}_{\text{SYK}} + \mathcal{S}_g$. We define the paring order parameter as

$$\Phi(\tau,x) = \frac{g}{N} \sum_{i=1}^N \langle \psi_{i,e}^{(1)}(\tau,x) \psi_{i,h}^{(2)}(\tau,x) \rangle, \quad (60)$$

which accounts for the pairing of electrons and holes in the different ladders. Next, one averages over the flavors and performs a decomposition of the fermionic fields in the SYK term into the Green's function $\hat{G}(\tau,x)$ and the self-energy $\hat{\Sigma}(\tau,x)$, which are to be found self-consistently with $\Phi(\tau,x)$. The decomposition of the additional interaction term \mathcal{S}_U can be done with the introduction of an auxiliary field $F(\tau,x)$ and the order parameter $\Phi(\tau,x)$,

$$\begin{aligned} \mathcal{S} = \mathcal{S}_0 + & \sum_{i,\alpha,\nu\nu'} \int_{\tau,x} \bar{\psi}_{i,\nu}^{(\alpha)}(\tau,x) \hat{\Sigma}_{\sigma\sigma'}^{(\alpha)}(\tau-\tau',x-x') \psi_{i,\sigma'}^{(\alpha)}(\tau',x') \\ & + N \int_{\tau,x} \left[F(\tau,x) \bar{\psi}_{i,e}^{(1)}(\tau,x) \bar{\psi}_{i,h}^{(2)}(\tau,x) + F^*(\tau,x) \psi_{i,h}^{(2)}(\tau,x) \psi_{i,e}^{(1)}(\tau,x) \right] + (1) \leftrightarrow (2). \end{aligned} \quad (61)$$

$$\begin{aligned} & - N \sum_{\alpha} \int_{\tau,\tau'} \int_{x,x'} \text{tr} \left[\hat{\Sigma}^{(\alpha)}(\tau'-\tau, x'-x) \hat{G}^{(\alpha)}(\tau-\tau', x-x') \right] \\ & - \frac{J^2 N}{2} \sum_{\alpha} \int_{\tau,\tau'} \int_{x,x'} \text{tr} \left[\hat{G}^{(\alpha)}(\tau-\tau', x-x)^2 \right] \text{tr} \left[\hat{G}^{(\alpha)}(\tau'-\tau, x-x)^2 \right] \end{aligned} \quad (62)$$

$$- \frac{2N}{g} \int_{\tau,x} F^*(\tau,x) \Phi(\tau,x) - \frac{2N}{g} \int_{\tau,x} F(\tau,x) \Phi^*(\tau,x) + \frac{2N}{g} \int_{\tau,x} \Phi^*(\tau,x) \Phi(\tau,x) \quad (62)$$

Considering the pairing term a weak perturbation, we assume that $\hat{\Sigma}^{(\alpha)} = \Sigma \sigma_z$ and $\hat{G}^{(\alpha)} = G \sigma_z$ has the same form as in the normal state. The integral over the ψ_i , $\bar{\psi}_i$ fields can be broken into N identical copies. Note that the symmetry of the model implies $\hat{G}^{(\alpha)} \hat{\Sigma}^{(\alpha)} = \hat{G} \hat{\Sigma}$. Integrating out the fermions, the partition function can then be written as $Z = \int e^{-N\mathcal{S}_{\text{eff}}}$ where the field integral

is over the remaining fields. The effective action becomes

$$\begin{aligned} \mathcal{S}_{\text{eff}} = & -2 \log \det \hat{A} + \frac{2}{U} \int_{\tau,x} \Phi^*(\tau,x) \Phi(\tau,x) \\ & - J^2 \int_{\tau,\tau'} \text{tr} \hat{G}^2(0, \tau-\tau') \text{tr} \hat{G}^2(0, \tau'-\tau) \\ & - 2 \int_{x,x'} \int_{\tau,\tau'} \text{tr} \left[\hat{\Sigma}(x-x', \tau-\tau') \hat{G}(x'-x, \tau'-\tau) \right] \\ & - \frac{2}{g} \int_{\tau,x} [F^*(\tau,x) \Phi(\tau,x) + F(\tau,x) \Phi^*(\tau,x)] \end{aligned}$$

where

$$\hat{A}[\Sigma, F] = \begin{pmatrix} G_N^-(i\omega, k) & F \\ F^* & G_N^+(i\omega, k) \end{pmatrix} \quad (63)$$

is a 2×2 matrix written in the reduced Nambu basis

$$\left(\psi_{i,e}^{(1)}(-i\omega_n, -k), \bar{\psi}_{i,h}^{(2)}(i\omega_n, k) \right), \quad (64)$$

where

$$G_N^\pm(i\omega_n, k) = \frac{k^2}{2m} - i\omega + \Sigma(\pm i\omega_n, \pm k) \quad (65)$$

is the corresponding normal state Green's function.

Assuming a uniform order parameter, the saddle point minimization of the action in Φ^* gives $F = \Phi$. The other Schwinger-Dyson equations follow from minimization with respect to Σ , G and F respectively,

$$\frac{G_N^-(i\omega_n, k) |\phi|^2 - G_N^+(i\omega_n, k) G_N^-(i\omega_n, k)^2}{(\det \hat{A})^2} = G(i\omega_n, k)$$

$$\Sigma(\tau, x) = -J^2 \delta(x) G(-\tau, 0) [G(\tau, 0)]^2, \quad (66)$$

and

$$\int_k T \sum_{\omega_n} \frac{2G_0^+(i\omega_n, k) G_0^-(i\omega_n, k) - |\Phi|^2}{(\det \hat{A})^2} = \frac{1}{g}.$$

Close to the phase transition, where $\Phi \rightarrow 0$, the first two Schwinger-Dyson equations recover the normal state set of equations (11) and (12), whereas the last one can be cast as

$$\int_k T \sum_{\omega_n} \frac{1}{(k^2/2m + \Sigma(i\omega_n))(k^2/2m + \Sigma(-i\omega_n))} = \frac{1}{g}. \quad (67)$$

The sum and the integral can now be performed numerically after expressing the self energy in terms of the scaling functions (37). In the strongly dispersive regime, $T \ll t^2/J$, this yields

$$T_c = c \frac{g^5}{(2m)^2 J^6}, \quad (68)$$

where

$$c = \sum_{\omega_n} \int_{-\infty}^{\infty} dz \frac{1}{\left| z^2 + F_\Sigma(\frac{\omega_n}{T_c}) \right|^2} \approx 5.5 \quad (69)$$

gives the numerical prefactor. In contrast, in the weakly dispersive case, for $t^2/J \ll T \ll J$, Eq. (67) becomes

$$T \sum_{\omega_n} \frac{1}{\Sigma(i\omega_n) \Sigma(-i\omega_n)} = \frac{1}{U}, \quad (70)$$

recovering the known result $T_c \approx (2J/\pi) \tan^{-1} e^{-\sqrt{\pi}J/g}$ [24].

VII. DISCUSSION

In this work, we studied a simple semimetallic version of a dispersive SYK model in one dimension. Contrary to most studies of dispersive models in the literature [13–17], we focus on a regime of infinite bandwidth, which is the stable fixed point of this problem. In this limit, we find that the Schwinger-Dyson equations do not admit an exact analytic finite temperature solution even in the IR approximation, where it is assumed that $\Sigma(i\omega) \gg i\omega$. In particular, the model does not exhibit conformal symmetry, which makes it difficult to solve the Schwinger-Dyson equations analytically. We solve those equations *exactly* exploiting the scaling symmetry of the model, combined with numerical calculations. We find that the Greens function and self-energy scale with temperature with a power law of $T^{-\frac{2}{5}}$ and $T^{\frac{4}{5}}$ respectively.

Using this solution to study transport properties, we show that dc resistivity scales with a sublinear power law dependence on temperature, $\rho \sim T^{\frac{2}{5}}$. We compute the Lorentz ratio $L = \kappa/(\sigma T)$ with the analytically continued scaling functions and find that $L \approx 3.2$, rather close to that of Fermi liquids. The scaling analysis of this problem indicates if one starts in the high temperature SYK fixed point of the problem, where $t^2/J \ll T \ll J$, the hopping parameter will grow as one scales the temperature down, while the SYK coupling is marginal. The scaling flows towards the strongly dispersive regime, where the Schwinger-Dyson equations indicate the presence of a distinct incoherent NFL regime at $T \ll t^2/J$. That contrasts with the behavior of incoherent metals, which have a finite Fermi surface. In the latter, the RG flows towards a Fermi liquid at low temperature [16].

Those results should be compared with the several lattice models of SYK dots that have been studied recently [13, 16, 17]. Ref. [13, 16] studied a lattice of coupled dots in the limit where the SYK coupling J is the highest energy scale. In those cases, the physics of a single dot dominates, with the effects of hopping being perturbative. The $\Sigma \propto \sqrt{\omega}$ scaling of the self energy in this limit ultimately leads to a linear in T dc resistivity.

Among these models, the one studied in Ref. [17] is the closest to ours. They examined a finite bandwidth model for arbitrary dimension and dispersion with a color site dependent SYK interaction, which forces the saddle point solution of the Green's function to be diagonal but still color site dependent. Their solution for the self-energy is purely imaginary and color site independent, differently from our results. That leads to an approximate conformal symmetry in the problem in the NFL regime, in contrast with our results, where we find that conformal symmetry is absent. In this work, we focused in the crossover between the regime dominated by the $0+1$ dimensional SYK fixed point and the low temperature NFL regime for a 1D semimetal with parabolic band touching, and addressed the transport properties of this novel state.

We also considered a bilayer system, comprising of two copies of the semimetallic 1D ladder model. We examined

the excitonic instability for a repulsive pairing electrons and holes living in different ladders. In metals, excitonic condensates require indirect exciton formation between states siting in Fermi surfaces of electrons and holes. Due to the absence of a Fermi surface and the large density at the touching point, even in the presence of disorder, indirect excitonic pairs can condense at finite tempera-

ture. We find that the condensation temperature in the NFL regime scales as a fast power law g^5/J^6 , where g is the strength of the repulsive coupling between the two layers.

Acknowledgements.— We thank Arijit Haldar for several helpful discussions. BU and GJ acknowledge Carl T. Bush fellowship and NSF grant DMR-2024864 for partial support.

[1] S. Sachdev, *Bekenstein-Hawking Entropy and Strange Metals*, Phys. Rev. X **5**, 041025 (2015).

[2] S. Sachdev and J. Ye, *Gapless Spin-fluid ground state in a random quantum Heisenberg magnet*, Phys. Rev. Lett. **70**, 3339 (1993).

[3] S. H. Shenker and D. Stanford, *Black holes and the butterfly effect*, JHEP 03 (2014).

[4] S. H. Shenker and D. Stanford, *Stringy effects in scrambling*, JHEP 05 (2015) 132.

[5] J. Maldacena, S. H. Shenker, and D. Stanford, *A bound on chaos*, JHEP 08 (2016)106.

[6] J. Maldacena, D. Stanford, and Z. Yang, *Diving into Traversable Wormholes*, Fortschr. Phys. 65, 1700034 (2017).

[7] M. Mitrano, A. A. Husain, S. Viga, A. Kogar, M. S. Rak, S. I. Rubeck, J. Schmalian, B. Uchoa, J. Schneeloch, R. Zhonge, G. D. Gue, and P. Abbamonte, *Anomalous density fluctuations in a strange metal*, Proc. Nat. Acad. Sci. **115**, 5392 (2018).

[8] A. A. Husain, M. Mitrano, M. S. Rak, S. Rubeck, B. Uchoa, K. March, C. Dwyer, J. Schneeloch, R. Zhonge, G. D. Gu, and P. Abbamonte, *Crossover of Charge Fluctuations across the Strange Metal Phase Diagram*, Phys. Rev X **9**, 041062 (2019).

[9] J. Zaanen, *Planckian dissipation, Minimal viscosity and the transport in cuprate strange metals*, SciPost Phys. **6**, 061 (2019).

[10] A. A. Patel and S. Sachdev, *Critical strange metal from fluctuating gauge fields in a solvable random model*, Phys. Rev. B **98**, 125134 (2018).

[11] P. Cha, N. Wentzell, O. Parcollet, A. Georges, and E.-A. Kim, *Linear resistivity and Sachdev-Ye-Kitaev (SYK) spin liquid behavior in a quantum critical metal with spin-1/2 fermions*, Proc. Natl. Acad. Sci. USA **117**, 18341 (2020).

[12] G.E. Volovik, *Flat band and Planckian metal*, JETP Lett. **110**, 352-353 (2019).

[13] A. A. Patel, J. McGreevy, D. P. Arovas, and S. Sachdev, *Magnetotransport in a model of a disordered strange metal*, Phys. Rev. X **8**, 021049 (2018).

[14] P. Zhang, *Dispersive Sachdev-Ye-Kitaev model: band structure and quantum chaos*, Phys. Rev. B **96**, 205138 (2017).

[15] X.-Y. Song, C.-M. Jian, and L. Balents, *Strongly Correlated Metal Built from Sachdev-Ye-Kitaev Models*, Phys. Rev. Lett. **119**, 216601 (2017).

[16] D. Chowdhury, Y. Werman, E. Berg, and T. Senthil, *Translationally Invariant Non-Fermi Liquid Metals with Critical Fermi-Surfaces: Solvable Models*, Phys. Rev. X **8**, 031024 (2018).

[17] A. Haldar, S. Banerjee, V. B. Shenoy, *Higher-dimensional Sachdev-Ye-Kitaev non-Fermi liquids at Lifshitz transitions*, Phys. Rev. B **97**, 241106 (2018).

[18] D. Ben-Zion and J. McGreevy, *Strange metal from local quantum chaos*, Phys. Rev. B **97**, 155117 (2018).

[19] A.A. Patel and S. Sachdev, *Theory of a Planckian metal*, Phys. Rev. Lett. **123**, 066601 (2019).

[20] P. T. Dumitrescu, N. Wentzell, A. Georges, and O. Parcollet, *Planckian metal at a doping-induced quantum critical point*, arXiv:2103.08607 (2021).

[21] A. Kogar, Melinda S. Rak, S. Vig, A. A. Husain, F. Flicker, Y. Il Joe, L. Venema, G. J. MacDougall, T. C. Chiang, E. Fradkin, J. van Wezel, P. Abbamonte, *Signatures of exciton condensation in a transition metal dichalcogenide*, Science **358**, 1314–1317 (2017).

[22] J. I. A. Li, T. Taniguchi, K. Watanabe, J. Hone and C. R. Dean, *Excitonic superfluid phase in double bilayer graphene*, Nat. Phys. **13**, 751 (2017).

[23] Ilya Esterlis, Jārg Schmalian, *Cooper pairing of incoherent electrons: An electron-phonon version of the Sachdev-Ye-Kitaev model*, Phys. Rev. B **100**, 115132 (2019).

[24] Aavishkar A. Patel, Michael J. Lawler, Eun-Ah Kim, *Coherent Superconductivity with a Large Gap Ratio from Incoherent Metals*, Phys. Rev. Lett. **121**, 187001 (2018).

[25] Debanjan Chowdhury, Erez Berg, *Intrinsic superconducting instabilities of a solvable model for an incoherent metal*, Phys. Rev. Research **2**, 013301 (2020).

[26] Y. Wang, *Solvable strong-coupling quantum-dot model with a non-Fermi-liquid pairing transition*, Phys. Rev. Lett. **124**, 017002 (2020).

[27] H. Wang, A. L. Chudnovskiy, A. Gorsky, A. Kamenev, *Sachdev-Ye-Kitaev superconductivity: Quantum Kramers and generalized Richardson models*, Phys. Rev. Research **2**, 033025 (2020).

[28] A. Georges, G. Kotliar, W. Krauth, and M. J. Rozenberg, *Dynamical mean-field theory of strongly correlated fermion systems and the limit of infinite dimensions*, Rev. Mod. Phys. **68**, 13 (1996).

[29] H. J. Vidberg, J. W. Serene, *Solving the Eliashberg equations by means of N-point Pade approximants*, J. Low Temp. Phys. **29**, 179–192 (1977).

[30] O. Parcollet, M. Ferrero, T. Ayral, H. Hafermann, I. Krivenko, L. Messio, and P. Seth, *TRIQS: A Toolbox for Research on Interacting Quantum Systems*, Comp. Phys. Comm. **196**, 398-415 (2015).